

Additive Manufacturing of Metal Bandpass Filters for Future Radar Receivers

Bradley Grothaus¹, Dane Huck¹, Austin Sutton¹, Ming Leu¹, Ben Brown²

¹Department of Mechanical and Aerospace Engineering, Missouri University of Science and Technology, Rolla, MO 65409

²Department of Energy's Kansas City National Security Campus Managed by Honeywell FM&T, Kansas City, MO 64147

Abstract

Selective laser melting (SLM) is a powder-bed fusion (PBF) process that bonds successive layers of powder with a laser to create components directly from computer-aided design (CAD) files. The additive nature of the SLM process in addition to the use of fine powders facilitates the construction of complex geometries, which has captured the attention of those involved in the design of bandpass filters for radar applications. However, a significant drawback of SLM is its difficulty in fabricating parts with overhangs necessitating the use of support structures, which, if not removed, can greatly impact the performance of bandpass filters. Therefore, in this study bandpass filters are manufactured in two stages with 304L stainless steel where each builds only a portion of the part to improve the reliability in manufacturing the overhangs present. The results show that the versatility of SLM can produce difficult-to-manufacture bandpass filters with high dimensional accuracy. This work was funded by Honeywell Federal Manufacturing & Technologies under Contract No. DE-NA0002839 with the U.S. Department of Energy.

1. Introduction

Powder-bed fusion (PBF) is a class of additive manufacturing (AM) techniques that refer to the selective consolidation of particles in a layer-by-layer fashion to create three-dimensional components. Among the PBF methods is the selective laser melting (SLM) process where a laser is used to weld regions of a powder-bed to construct parts additively. With the number of increasing applications of SLM in industries including aerospace and medical fields, the amount of research being directed towards improving the process regarding manufacturability of geometrically complicated components has increased dramatically in the previous 10 years. Moreover, the types of materials manufacturable by SLM has increased to encompass primarily aluminum, titanium, nickel, and steel alloys so that the parts fabricated may be used in service.

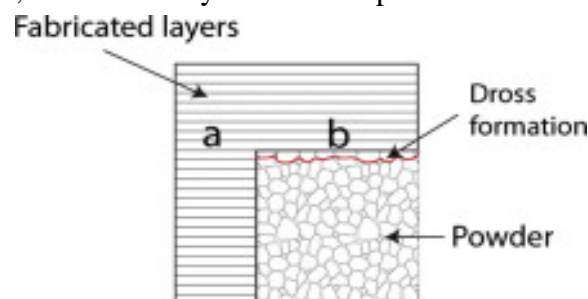


Figure 1. Illustration of overhang and dross formation [1]

Although SLM has enabled more freedom in the design process due to its ability for constructing complex geometry, this method still suffers from the difficulty in printing overhanging structures, often necessitating the use of supports that may be difficult to remove. During the SLM process, high temperatures exist above the melting point of the metal material being processed [2]. Subsequent rapid solidification occurs which causes the formation of residual stresses, which can distort parts. Therefore, supports in SLM serve two main purposes: anchoring the solidified material to the substrate to eliminate part distortion due to residual stresses, and heat dissipation. If parts are not properly supported, the concentrated heat cannot be sufficiently dissipated through the powder bed due to its low conductivity [3], causing thermo-elastic distortion [1]. This problem is exacerbated for components that are built less than 45 degrees relative to the substrate, requiring support material to be inserted to ensure that the parts can be built [4]. Under this critical angle the melt pool increases and flows into the powder bed because of gravity and both the capillary forces and thermal energy cause the underlying powder to adhere to the part surface causing warping and drastically increasing the surface roughness leading to what is more commonly known as dross formation [1], as shown in Figure 1. Many times, dross formation can cause harm to the recoater jeopardizing an entire build and the dimensional accuracy of the part. Thus, these support structures become almost essential to parts built at low angles, thereby forcing geometric constraints to be applied to parts during the design process so that they may be correctly manufactured by SLM.

In the case of bandpass filters for use in radar applications, these geometric constraints can greatly inhibit the applicability of SLM for their construction. However, as SLM can produce complicated geometry, the process has the potential to manufacture unique designs that are difficult to produce by conventional means. The bandpass filters of interest for this study are an interdigitated design, which are shown in Figure 2. The bandpass filters on the left and right in Figure 2 are hereby referred to as bandpass filter A and B, respectively. It should be noted that such both geometries are difficult to produce by conventional means as the small cantilevers can become distorted during the milling process influencing the performance of the bandpass filter, which can be avoided using SLM. Yet, the interdigitated cantilevers are still difficult to manufacture with SLM as they produce overhangs regardless of the orientation at which the parts are built. Thus, the parts pose a serious challenge in the SLM process, which serves as the basis of this paper.

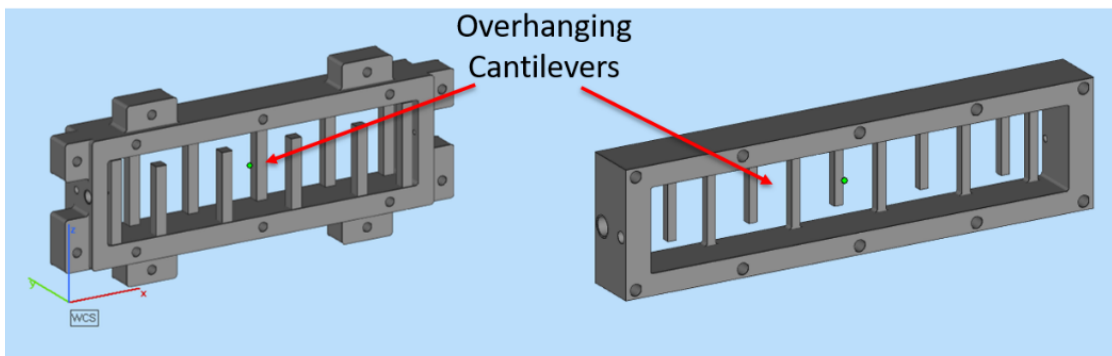


Figure 2. CAD models of two bandpass filter designs (not to scale).

The goal of this research is to explore and evaluate methods implementable in the SLM process for fabrication of the given parts with a Renishaw AM250 and assess each in terms of their success with respect to dimensional accuracy and overall manufacturability. The most popular method for building these overhang structures is using supports. However, support structures can affect the SLM process in undesirable ways. The need for support structures increases the laser exposure time during the process and the removal of these structures can take a significant amount time and energy ultimately increasing the cost. Therefore, in addition to building each of the parts with supports, an alternative method is presented where only a portion of each part is built at a time to bypass the manufacture of overhanging structures, hereby referred to as “flip and fixture.” Lastly, an additional technique is used, which involved the use of non-contact supports, a common technique employed in electron beam additive manufacturing. With non-contact supports, supports are offset a certain distance from the parts to provide heat dissipation without adhering to the part surface for ease of removal.

2. Method 1: Optimization of Supports (Unsuccessful)

A common choice for difficult-to-manufacture parts in SLM is to build supporting material that will assist in fabrication. This procedure is often coupled with orienting the parts in an optimized manner that will minimize the amount of support material needed and facilitate the ease of their removal to retain the final part. Other concerns when using support material include minimization of surface roughness and dimensional accuracy, both of which are greater in SLM for overhanging surfaces due to dross formation. Thus, optimizing the support structures to mitigate all these negative effects is crucial.

In the support optimization process performed in Materialise Magics, the goal was to produce structures with limited volume, small areas of connection to the part (to make the removal process easy and time-efficient) while orienting the part optimally for a good surface finish and limit down-facing surfaces. In this study there were five different parts on the support optimization build plate, each with a different set of support and orientation combinations. Elements that varied

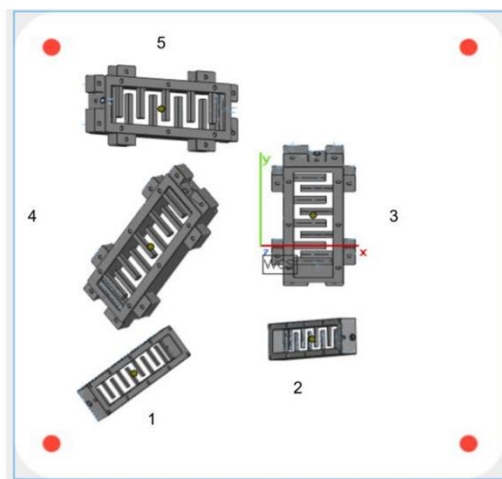


Figure 3. Method of support plate overhead view

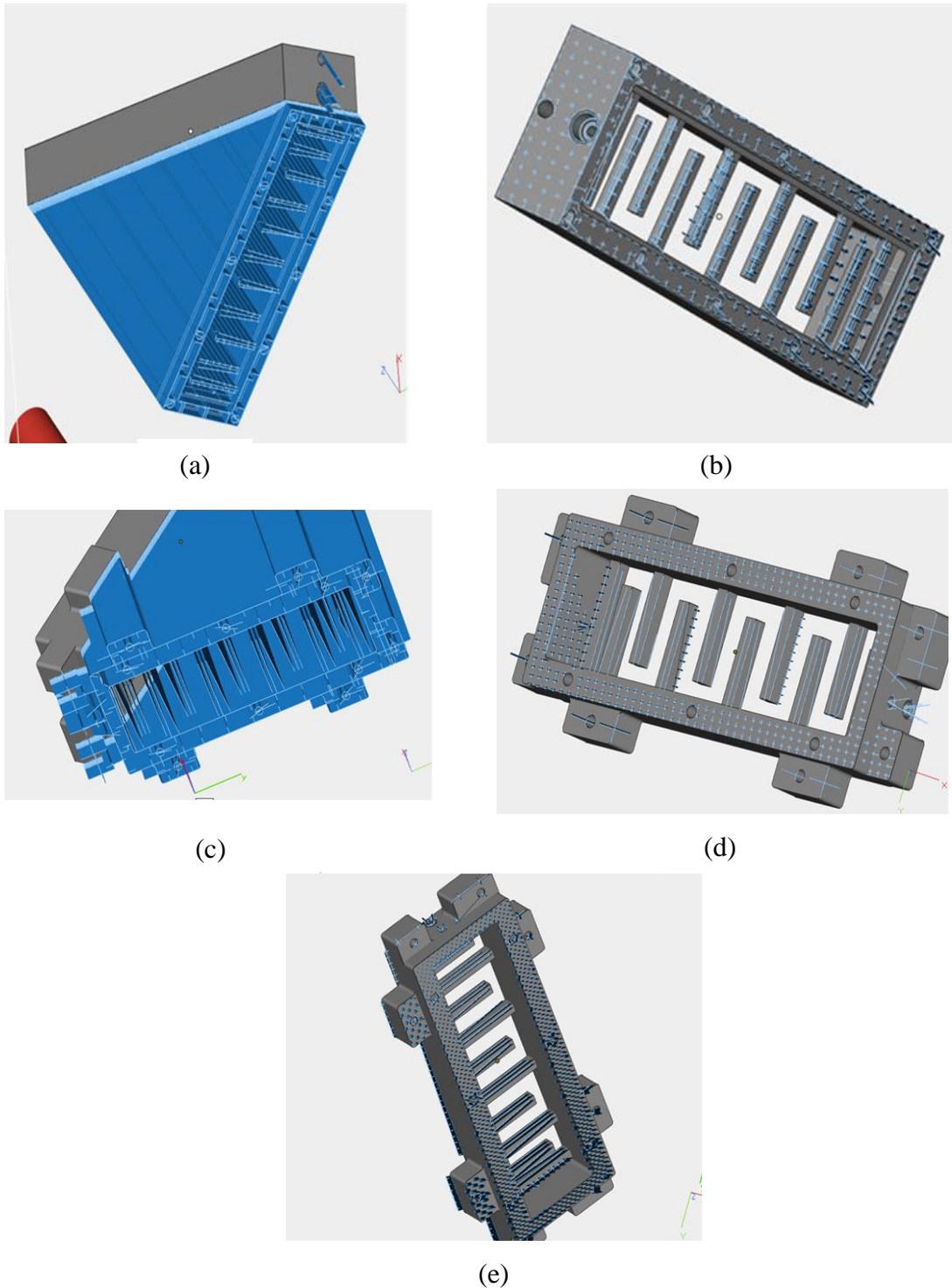


Figure 4. Support optimization as performed in Materialise Magics for the two bandpass filters in this study: (a) line supports with orientation pertaining to minimal support surface, (b) point supports at 60 degrees from the horizontal, (c) line supports at 45 degrees from the horizontal, (d) point supports with minimal support surface and z-height, and (e) point supports with minimal support surface.

with each part were the orientation and the type of support used, either a line support or a point

support. A line support is a wall of support material with perpendicular struts, while a point support simply attaches to the part at a single location. When using point supports, many were generated to simulate a “wire brush” for ease of removal. To further enhance the ease of removal, each type of support was only welded with one laser pass making them weak due to the porosity present without remelting. To attempt different orientations for each part, the optimization tool in Materialise Magics software was utilized. This tool optimizes the orientation based off the geometry and down facing surfaces to create an orientation that will limit supports and laser exposure time. The other orientations (besides the Materialise Magics optimized orientation) used were 45 and 60 degrees. On all the parts the teeth of the supports (the very top and bottom of the supports that connect to the substrate and the component being supported) were designed to be easily removed and quick to build as was found by Calignano [5]. Also, on each cantilever there were two line supports added to support each downfacing edge of the cantilever. The supports generated for each part can be seen in Figure 4.

Part 1 was built with all line supports and the orientation was optimized to minimize the amount of support surface needed on the part (Figure 5a). This was the most successful part built. It finished building to completion and is recognizable as the part it is supposed to be. Unfortunately, the down-facing surfaces have a less than optimal surface finish and low dimensional accuracy.

Part 2 was built with point supports, and the orientation was 60 degrees vertically from the horizontal build plate. This part failed early on due to the cross teeth in supports for the cantilevers overlapping. Due to this overlapping, the laser beam passed multiple times over the same section of each cantilever causing distortion. So as not to interfere with the recoater, this meant the part had to be suppressed early in the build.

Part 3 was built with line supports and the orientation was 45 degrees vertically from the horizontal build plate. This part failed as soon as the sections with a 45-degree angle without supports started building. When this occurred the part had to be suppressed.

Part 4 was built with the point supports, and the orientation was optimized in the Materialise Magics surface to optimize supports and the build height. This part failed to build to completion (Figure 5b). As it was building the angle was close to the critical angle and was close to failing but the machine would correct itself before the part failed. When it reached the top, it did not correct itself therefore it had to be suppressed before completion. Even with most of the part that did complete, the surface finish on the down facing surfaces was not optimal.

Part 5 was built with point supports, and orientation was optimized in the Materialise Magics surface to minimize the amount of support surface on the part. This part failed to build to completion. Just as Part 3 on this build plate did, it failed when it started building the opposite angled non-supported parts.

3. Method 2: Non-Contact Supports (Unsuccessful)

Another method that was examined in this research was the non-contact support method. The main purpose in evaluating this method an alternative means of building simple cantilever



Far Left: Part
viewed in
Materialise Magics
Software

Top: Up facing
surface



Bottom: Down
facing surface

(a)



Far Left: Part
viewed in
Materialise
Magics
Software

Top: Up facing
surface



Bottom: Down
facing surface

(b)

Figure 5. Fabricated bandpass filters with (a) line supports and minimal support surface, and (b) point supports with minimal support surface and z-height.

overhangs in the SLM process. Unlike conventional support structures, non-contact supports are completely separated from the overhang by some gap distance. The idea is that the support will act as a heat sink and help with thermal dissipation via heat conduction. Ideally, this would lead to the overhang building without the usual distortion of the overhang occurring such as when there is no support at all. Related previous research consists of one study examining the feasibility of non-contact supports in the electron beam melting process [6]. Figure 6 illustrates the concept of the non-contact support. Note that the overhang is completely horizontal. This is the orientation of the overhangs tested throughout the method of non-contact supports.

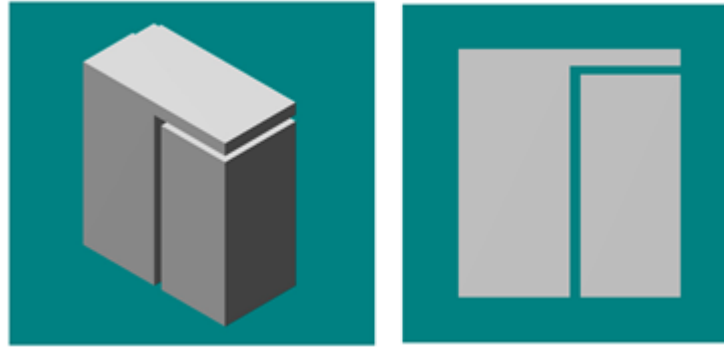


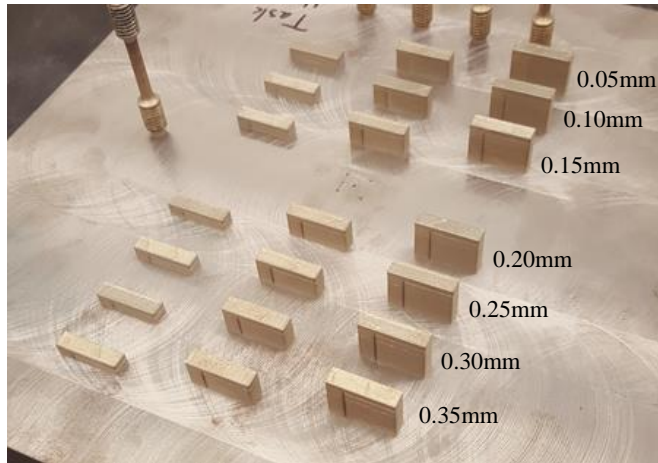
Figure 6. Non-contact support with overhang CAD model.

The experimental approach for testing the method of non-contact supports consists of the following: design the test setup, build the test setup, and observe the result of each test. Each test is essentially a set of cantilever overhang structures. Each test structure contains an overhang with a base and a block under the overhang. The block is separated by some gap distance from the overhang. After each test was examined, observations were drawn, and a new test was designed to make more observations.

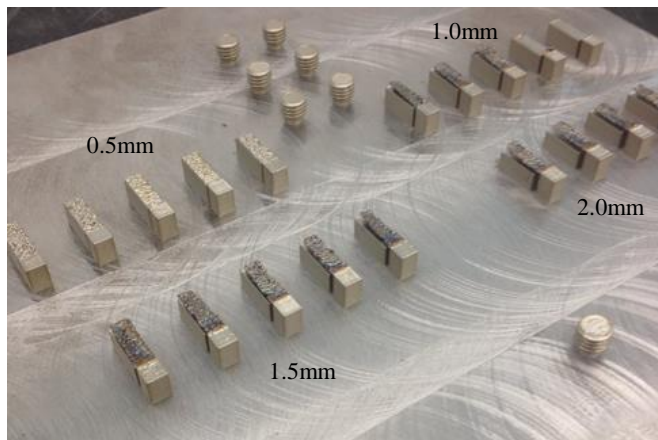
For the first test setup, the questions to consider include: the required gap distance that would be successful, if any, and whether the thickness of the non-contact support carries any effect. This led to a test setup that was used to evaluate multiple variables. The set of tests consisted of three different heights of overhang test structures, each having a gap distance from 0.05mm to 0.35mm (0.05mm interval jumps). These results are shown in Figure 7a. All the test structures from the previous test bonded between the overhang and the non-contact support. The second set of tests consisted of five iterations of each gap distance of 0.5mm, 1.0mm, 1.5mm, and 2.0mm. The five iterations made it possible to see any consistency or lack thereof within each gap testing and the larger gap intervals allowed for more rapid locating of a precise range for building overhangs. The test results are shown in Figure 7b.

The third and final test was that of a more specific range of gap distance. Given that the largest three gaps of the previous test failed to build, and the smallest gap caused bonding between the overhang and the support, it appeared that the range was between 0.5mm and 1.0mm. Staying close to the smaller end of the range, and including some overlap, the next setup consisted of a similar outline. Again, five iterations of each gap distance were tested: 0.4mm, 0.5mm, 0.6mm, 0.7mm. The results are shown in Figure 7c.

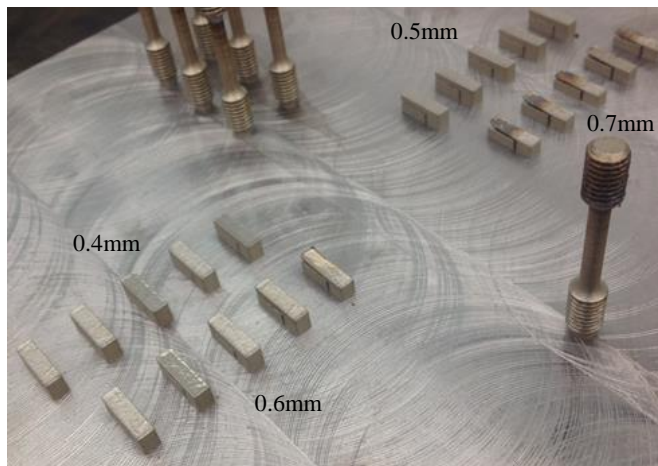
Three different outcomes occurred from these tests, as illustrated in Figure 8. For this method to be feasible, there needs to be another outcome between bonding and curling: building successfully without curling. Unfortunately, the non-contact supports simply do not disperse fast enough for a successful build of an overhang. While the quality is better than the case where the horizontal overhang has no support whatsoever, it is not sufficient enough to build with dimensional accuracy and quality surface finish.



(a)



(b)



(c)

Figure 7. Non-contact support builds where (a) is the first set of tests, (b) is the second set of tests, and (c) is the third set of tests; the gap used is labeled next to each set of overhangs.

Table 1 shows that 0.6 mm and 0.7 mm converge to a single curling result for each. The 0.6 mm test overhangs had four that bonded, while the 0.7 mm test overhangs had four that failed

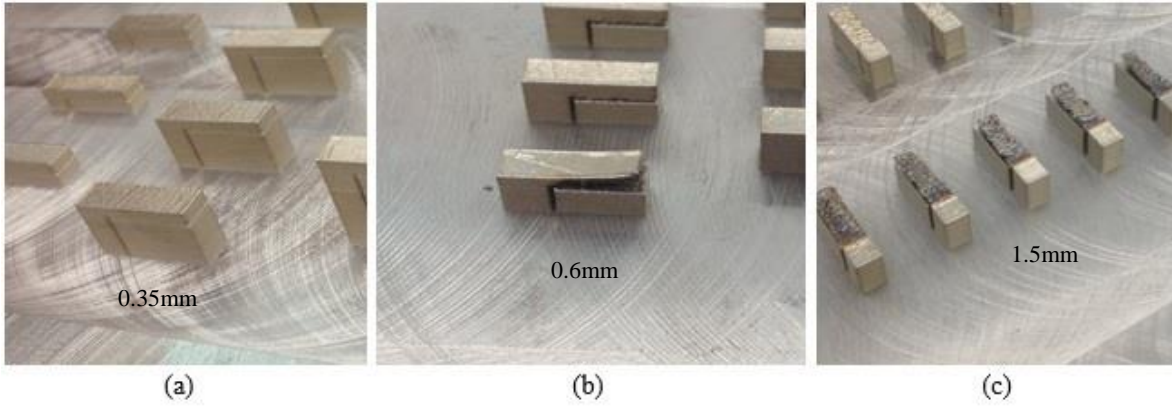


Figure 8. Three observed outcomes exhibited by the test overhangs: (a) bonding, (b) curling, and (c) failure to build.

to build. This hints at a gap distance between 0.6 mm and 0.7 mm, where the test overhangs would curl as depicted in Table 2. Curling is still not desirable, but an outcome that is closer to successfully building. Further testing would be needed to investigate the effect of gap distance on the build quality.

Table 1: Test Observations with frequency in the test.

Test #	Gap (mm)	Observation		
		Bonded	Curled	Failed
1	0.05	3		
	0.10	3		
	0.15	3		
	0.20	3		
	0.25	3		
	0.30	3		
	0.35	3		
2	0.5	5		
	1.0			5
	1.5			5
	2.0			5
3	0.4	5		
	0.5	5		
	0.6	4	1	
	0.7		1	4

Table 2: Fabrication results for different gap distances.

	Gap Range (mm)		
	$d < \sim 0.6$	$0.6 < d < 0.7$	$d > \sim 0.7$
Result:	Bonding	Curling	Failure to build

d = Gap distance

4. Method: Flipping and Fixturing (Successful)

The next method attempted was one that is termed as “flipping and fixturing,” as shown in Figure 9. The general idea is to divide the part with a horizontal cut into two sections that are both void of any problematic overhang. The first step in the fabrication would be to print out the larger of the two sections on a build plate as how normally a part would be printed, and when it is completed the built section would be flipped over, fixtured back onto the build plate where the other section would then be printed on top of it. While a novel idea this potential method came with potential issues and concerns that had to be overcome before the theory could be tested. For testing purposes, the bandpass filters were modified by removal of the holes to facilitate their manufacturability in SLM, and is hereby referred to as the proof-of-concept pieces.

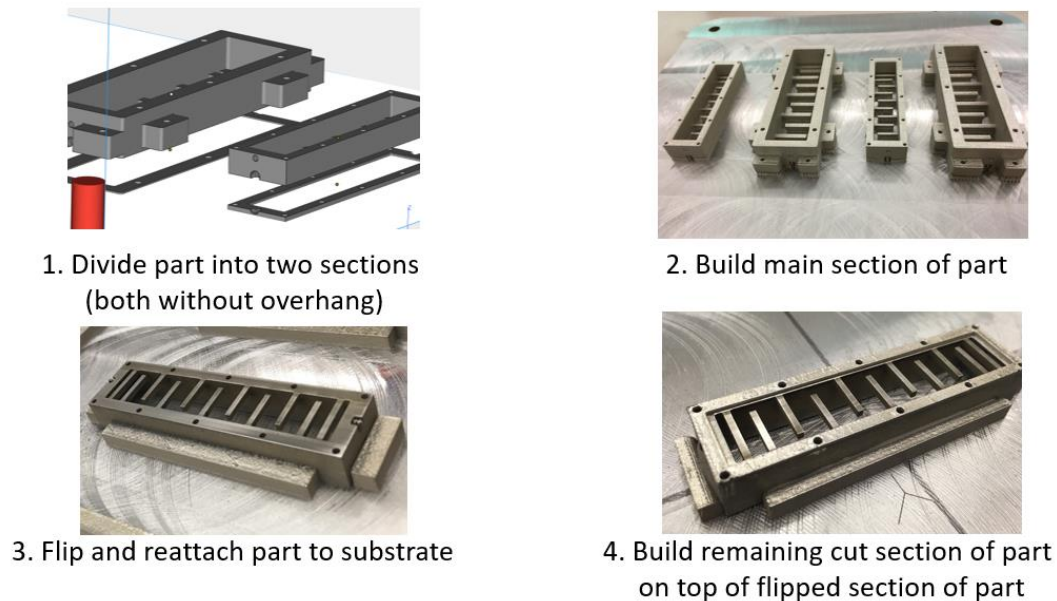


Figure 9. Illustration of flipping and fixturing method

The first problem needed to be solved was how the first section of the part will be fixtured to the substrate for the other section to build on top of it. Early ideas included adding a support structure on top of the part similar to the one on the bottom of it so when flipped it would be possible to align the location of the builds. Another idea contemplated was using an adhesive such as soldering or an epoxy. Past the issue of fixturing it to the plate is making sure the fixture is

centered and is exactly even in the z-direction as well. Ideas for this problem include coordinate mapping the build plate and centering on the previous build plate. One way to do that would be to create no build zones (parts in Materialise Magics that cannot be built over) with geometry of cut parts on top of where the old builds were as to keep the same alignment and centering. The latest and most executable ideas center around using guiding blocks to center the part. Other ideas have been investigated but not yet experimented such as the “hole” and “screw” methods. The last concern is the quality of bond that will be created after fixturing and flipping. In the study only one method has been attempted, i.e., use of guiding blocks.

4.1 Guiding Block Approach

Under the flipping and fixturing technique, the cut part is built regularly first. Then a second build plate with the guiding blocks outlining the part is built. The cut part is then flipped over and placed into the blocks that act as guiding blocks to center the part. Then using the same coordinates from the guiding block build plate, the rest of the build is completed on top.

4.2 Part Measurements

Before using the guiding block method to fixture the parts to the build plate it was necessary to determine the distance between the blocks and the part that should be allowed. As the parts’ melt pools expand the components slightly it is necessary to put some distance between the part and the block. Measurements were taken using stainless steel calipers corresponding to the dimensions depicted in Figure 10. Each part was measured in five spots for the total width, four

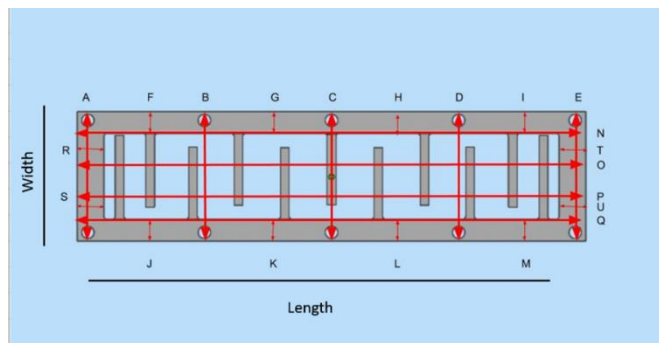


Figure 10. Locations of the measurements taken of the printed part using the flipping and fixturing method.

spots the total length, four spots each for the width of the bottom and top, and two spots each for the width of the left and right.

The measured results are given in Table 3. The numbers in the table indicate that the widths of the sides are on average 0.0052 mm larger than the CAD dimensions and all the differences were positive, meaning all the sides were wider than the CAD dimensions. The total lengths and widths are on average only 0.0059 mm larger than the CAD dimensions.

Table 3: Measurements of bandpass filters compared to the CAD dimensions.

Bandpass Filter A			
	CAD Dimensions (mm)	Avg. of Meas. (mm)	Differences(mm)
Length	86.58	86.5852	0.0052
Width	30.15	30.1564	0.0064
Bandpass Filter B			
Length	73.46	73.4653	0.0053
Width	18.84	18.8468	0.0068

4.3 Proof of Concept Trial

Using the guiding block method on the proof of concept part with trial distances between the part and guiding block of 0.005 mm, 0.05mm, and 0.1 mm, the proof of concept part was able to be flipped and fit into each set of guiding blocks. To fit the part into the 0.005 mm guiding block the top of the part (before flipped) needed to be sanded and hammered to fit inside. The 0.1mm guiding block was too loose and no part was attempted in that guiding block.

To level the parts vertically, minor sanding was done to ensure there were no errors when printing. An artificial powder bed was made by lowering the elevator and pouring in powder manually then slowly (0.05 mm at a time) raising the elevator until the part was detected visually. Then ensured the wiper would be able to distribute the powder evenly over the flipped parts. In this trial a build of 2 mm (Figure 11) was printed on top of the cut parts.

The trial part was built to completion and the bond evaluated. To evaluate the bond a 5 mm section of the side wall was removed by EDM. Then the removed sample piece was mounted and polished to a 1 μ m finish. At this point the sample piece was evaluated under a microscope. Before another microscopic evaluation the sample piece was etched using a 60% HNO₃, 40% H₂O solution. After microscopic evaluation, Vickers hardness tests were completed.

The guiding block method produced the parts with acceptable geometric accuracy and surface finish. The alignment was off by a very slight amount and was more precise in the part with 0.005 mm distance between the guiding blocks than the part with 0.05 mm distance.

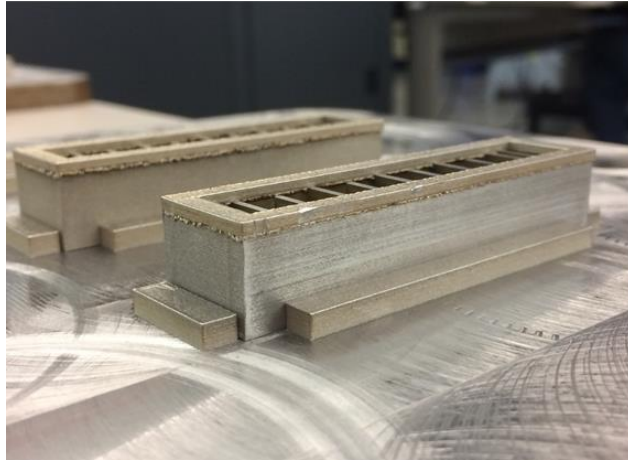


Figure 11. The proof of concept part after completion using the guiding block method.

When evaluating the bond there was no noticeable faults when examining under the microscope at the bond before the etch was completed. After etching the part, the bond area was very distinguishable as the melt pools are visible under microscope and the bond is in the location where the melt pools flip because the part was flipped (Figure 12). Looking at this bond under microscope after etching gave no indication of fault or sign of a bond that was not viable. The Vickers Hardness test gave results indicating the bond was no different from the bonds in the standard SLM part (Figure 13).



Figure 12. Both sides of bond area of sample piece observed under microscope (5X) after etching

4.4 Guiding Blocks with Actual Parts

With what was deemed as successful results with the proof of concept build the guiding block method was implemented with the actual bandpass filter designs. Considering the

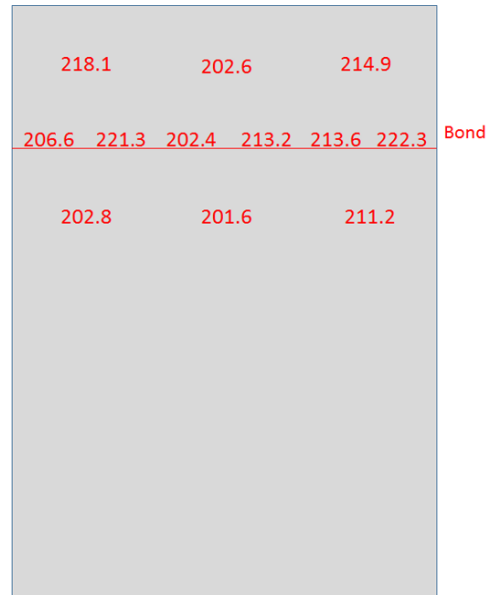


Figure 13. Graphic of sample with Vickers hardness values in the general area they were taken.

measurements previously taken as well as the proof of concept results distances of 0.005 mm, 0.01 mm, and .05mm between the part and the blocks were tested to find the best balance of efficiency and dimensional accuracy. While possible, positioning the edges was increasingly difficult with the smaller distances between the guiding block and part. To combat this problem a new guiding block design was implemented where the edges that line up with edges of the part were filleted as to make it easier to wedge the part into guiding blocks with smaller distances between the part and the blocks. With this newly designed block the bandpass filter designs are able to be fit inside very tight (0.01mm) guiding blocks in approximately three minutes with average human strength hammering of a rubber mallet.

With the newly designed guiding blocks the same process as was trialed with the proof of concept was tested. The resulting parts were produced with visible acceptable geometric accuracy and surface finish. The alignment visibly was seemingly perfect and much more precise than the proof of concept. To test this alignment a CMM (Coordinate Measurement System) was used. This machine tracks the x, y, and z coordinates every time the sensor contacts the part being measured. Taking over 600 coordinate points with this machine and using a MATLAB script, a three-dimensional rendering of the part can be made. To judge the surface finish and alignment a best fit line of all the points on each side is made and the coefficient of determination (R^2) value is determined. This value calculates the how close the data are to the best fit line from zero to one-hundred percent. The average of these value for the low frequency filter was 0.98, which indicates that the alignment is almost perfect.

As with the proof-of-concept trial, the bond was evaluated by using an EDM to remove a sample piece to be mounted and polished to 1 μm finish. At this point the sample piece was looked at under microscope to be evaluated. Before another microscopic evaluation the sample piece was

etched using a 60% HNO₃/40% H₂O solution. After microscopic evaluation Vickers hardness tests were completed.

When evaluating the bond there were no noticeable faults when looking under the microscope at the bond before the etch was completed. After etching the part, the bond area was very distinguishable as the melt pools are visible under microscope and the bond is in the location where the melt pools flip because the part was flipped. Looking at this bond under microscope after etching gave no indication of fault or sign of a bond that was not viable (Figure 14).

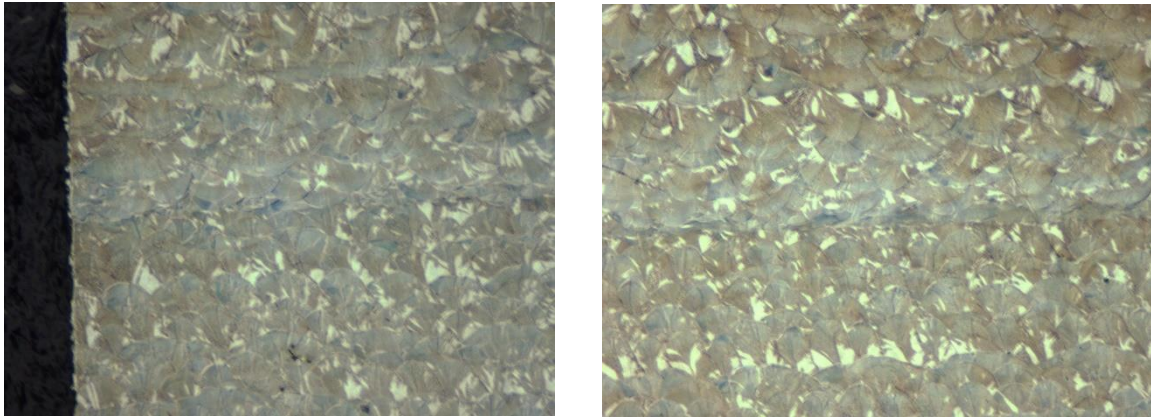


Figure 14. Both sides of bond area of sample piece looked at under microscope (5X) after etching

Differing from the proof of concept where Vickers hardness tests were only completed around the bond area, with the actual part the tests were completed evenly in a 500 by 500 grid throughout the whole cross-sectional area to test if any trends were evident. Creating a color map of the area it is evident there are no trends as the hardness values all fall within 40 units indicating again that bond is viable; see Figure 15.

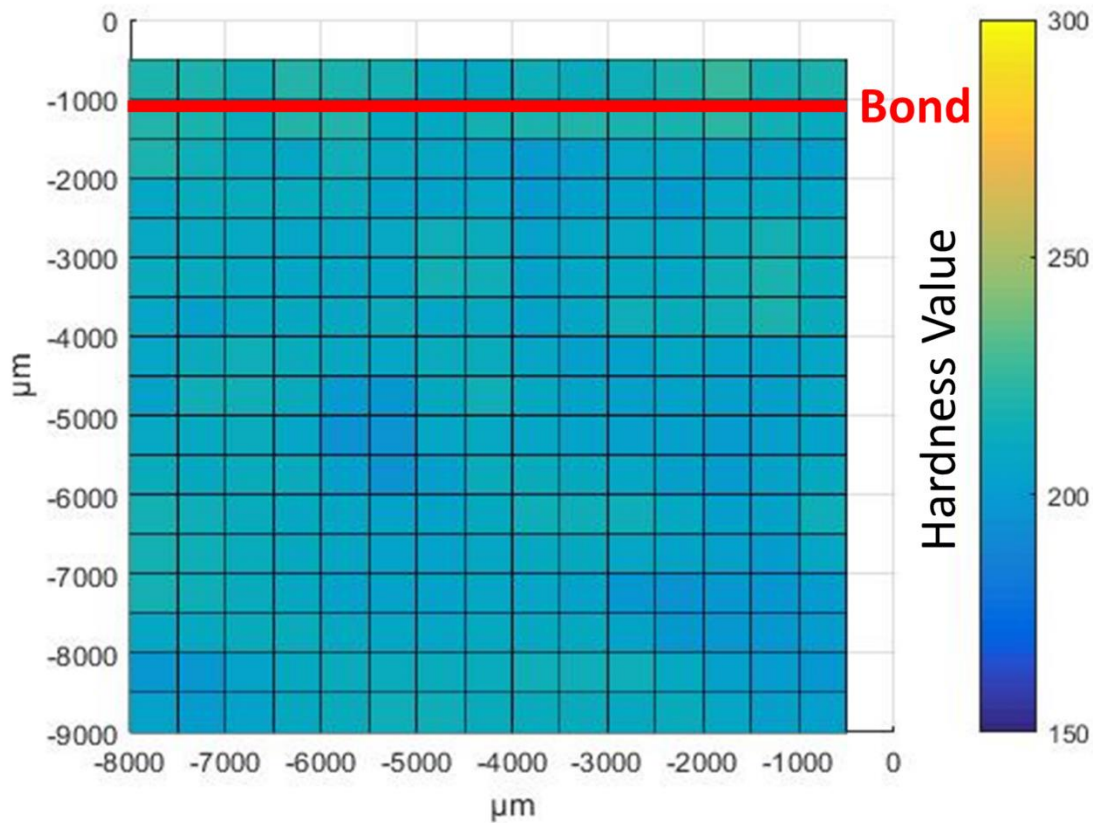


Figure 15. Vickers Hardness test result

5. Conclusions

The work in this study proves that interdigital bandpass filters can be printed in the SLM process although they are difficult to manufacture due to the overhangs present. Generation of optimal support material to aid in the construction of the filters was found to be unsuccessful due to the undesirable part distortion during fabrication and the large surface roughness of the downfacing surfaces. While non-contact supports do appear to have potential in alleviating the distortion encountered, the surface roughness will undoubtedly be present on the downfacing surfaces greatly influencing the performance of the bandpass filters. The solution implemented in this work for overcoming the manufacturing challenges of building overhangs in SLM involved flipping and fixturing, where only a portion of the bandpass filters are printed at a time to bypass building the overhangs. This technique proved to be dimensionally accurate while still maintaining acceptable bond quality at the interface.

Acknowledgement

This work was funded by Honeywell Federal Manufacturing & Technologies under Contract No. DE-NA0002839 with the U.S. Department of Energy. The United States Government retains and

the publisher, by accepting the article for publication, acknowledges that the United States Government retains a nonexclusive, paid up, irrevocable, world-wide license to publish or reproduce the published form of this manuscript, or allow others to do so, for the United States Government purposes.

References

- [1] F. Calignano, “Design optimization of supports for overhanging structures in aluminum and titanium alloys by selective laser melting”, *Materials & Design*, Vol. 64, 2014.
- [2] Gedda, H., Powell, J., Wahlström, G., Li, W.-B., Engström, H. and Magnusson, C. (2002), “Energy redistribution during CO2 laser cladding”, *Journal of Laser Applications*, Vol. 14, pp. 78-82.
- [3] Sih, S.S. and Barlow, J.W. (2004), “The prediction of the emissivity and thermal conductivity of powder beds”, *Particulate Science and Technology*, Vol. 22, pp. 427-440
- [4] Michael Cloots, Livia Zumofen, Adriaan Bernardus Spierings, Andreas Kirchheim, Konrad Wegener, (2017) "Approaches to minimize overhang angles of SLM parts", *Rapid Prototyping Journal*, Vol. 23 Issue: 2, pp.362-369, <https://doi.org/10.1108/RPJ-05-2015-0061>
- [5] Wang, D., Yang, Y., Yi, Z. and Su, X. (2013), “Research on the fabricating quality optimization of the overhanging surface in SLM process”, *The International Journal of Advanced Manufacturing Technology*, Vol. 65, pp. 1471-1484.
- [6] Cooper, Kenneth; Steele, Phillip; Cheng, Bo; Chou, Kevin. 2018. "Contact-Free Support Structures for Part Overhangs in Powder-Bed Metal Additive Manufacturing." *Inventions*, Vol 3, no. 1: 2.